RSC Advances

ROYAL SOCIETY OF CHEMISTRY

www.rsc.org/advances

Effect of Nanosilica-Based Immobile Antioxidant on thermal oxidative degradation of SBR

Haitao Wei, Lili Guo, Jing Zheng, Guangsu Huang and Guangxian Li

Abstract:

A new kind of nanosilica-based immobile antioxidant (RT-silica) consisting of nanosilica, antioxidant intermediate p-aminodiphenylamine (RT) and silane coupling agent 3-glycidoxypropyltrimethoxysilane (KH-560) was successfully synthesized via grafting reaction in our laboratory. It was revealed that the anti-oxidation performance of SBR/RT-silica composite was far superior to that of SBR/silica composite, especially at high temperature, based on the results of non-isothermal oxidation induction time (OIT) tests. The calculations of protection factors (PF) based on two non-Arrhenius temperature functions showed that silica possessed acceleration effect on the aging of SBR matrix. According to the results of tensile tests, SBR/RT-silica composites exhibited more preeminent mechanical property and residual rates during accelerated aging, in comparison with SBR/silica composites. The affections of RT-silica on the cross-linking network of SBR matrix were investigated via tube model, demonstrating that RT-silica can't change the cross-linking density, but can induce the chain entanglement of rubber molecular chains. Moreover, the calculated values of degradation activation energy of SBR composites via Kissinger–Akahira–Sunose (KAS) method and Friedman method showed that RT-silica changed the thermal-oxidative aging mechanism of SBR matrix.

Introduction

Since styrene–butadiene rubber (SBR) was successfully industrialized, it has been widely used because of its numerous excellent properties such as fabricability and usability. Although the abrasive resistance, heat-resistant quality and aging-resistant performance of SBR are better than those of natural rubber, the double bonds and allyl-hydrogen groups on SBR molecular chains make the rubber aging more likely in thermal or humid conditions. Besides, SBR does not belong to self-reinforcing rubber, because its segments lack short-range regular arrangement and form no paracrystalline structure during service life. The tensile strength of vulcanized SBR is only about 3 MPa, resulting in that SBR needs to be reinforced before use [1].

In order to cover the shortages of SBR, rubber antioxidants, such as 4010-NA and 4020, and reinforcing fillers, say carbon black and silica, were used to improve the usability of SBR. In the tire industry, both silica and carbon black (CB) can serve as reinforcing fillers, whereas silica can improve the abrasion resistance and tear strength of SBR matrix more significantly than carbon black. In particular, the rolling resistance of SBR/silica tire product is far lower than that of tire product prepared by SBR/CB composite [2]. Unfortunately, the concentration of traditional low-molecular-weight amine antioxidants will decrease in service due to its volatility and extractability, leading to the reduction of service life of SBR [3, 4]. In addition, as the poor dispersity of silica in rubber matrix resulting from the high surface energy of silica severely degrades the rubber performance, it’s necessary to change the surface polarity of silica from hydrophilicity to lipophilicity via surface modification, which

can improve the dispersity and reinforcement performance of silica in rubber matrix [5-10].

With the purpose of overcoming the drawbacks of rubber antioxidant, Ismail et al. prepared polyaniline which was one kind of high molecular weight antioxidant. Even though the polyaniline antioxidant possessed more effective anti-oxidation performance than traditional aniline antioxidant, it still volatilized at some extent in harsh conditions [11]. However, an even more promising method is grafting the antioxidant onto the polymer chain or solid filler. For example, H. Baharvand grafted the IPPD antioxidant onto the surface of clay, and then incorporated the modified clay into SBR matrix. It was found that the modified clay showed more excellent reinforcement and anti-aging performance than general clay in SBR matrix [12]. Therefore, we synthesized one new kind of nanosilica-based immobile rubber antioxidant (RT-silica) which aimed at restricting mobility of antioxidant. The grafted antioxidants can act as surface modifying agents for silica. Nanosilica as a potential silica filler has attracted more and more attention owing to its stability and large surface area. In this grafting reaction, the large surface area of nanosilica makes the effective contact area between silica and KH560 larger so that the antioxidants are easy to be fixed on the surface of nanosilica. In our previous paper, the structure of RT-silica has been confirmed via FTIR test, and the grafting efficiency of the grafting reaction was investigated via TGA [13]. The results of SEM and DSC tests revealed that RT-silica possessed better dispersibility, anti-oxidation performance and anti-migratory efficiency compared with the corresponding low molecular

counterpart (4010NA) [13]. However, the mechanical property, thermal-oxidative aging behavior and degradation kinetics of SBR/RT-silica composites still need to be investigated in more depth.

Oxidation induction time (OIT) and oxidation onset temperature (OOT) obtained from Differential Scanning Calorimetry (DSC) tests can accurately estimate the stability of SBR composites [14]. The longer OIT and the higher OOT mean the better stability of SBR composites. Šimon P et al. studied the oxidation induction period of materials via DSC and found that non-isothermal DSC measurement can determine OOT more accurately than isothermal DSC measurement [15, 16]. Furthermore, the OIT value at certain temperature can be calculated from the records of non-isothermal DSC tests at different heating rates [15, 16]. Then the protection factor (PF) as a common parameter of measuring the anti-aging efficiency of compounds can be calculated from the OIT value via the non-Arrhenius temperature function [17, 18].

In recent years, thermal analysis kinetics have been widely used across multiple industries for various applications, such as the prediction of service life of material, the evaluation of stability of medicine and the estimation of risk of explosives [19, 20]. Thermal analysis kinetics can be used to acquire the degradation activation energy of material via the reaction dynamic equations, such as Kissinger-Akahira-Sunose (KAS) equation and Friedman equation. The higher the degradation activation energy of material is, the better the thermal stability of material is [21]. J.Kuljanin-Jakovljevic et al. applied KAS method to calculate the

degradation activation energy of PS/Cds composites, revealing the change trend of degradation activation energy with the content of Cds [22].

Among lots of models which can be used to study the cross-linking network of rubber, tube model which takes the topological restriction and entanglement of molecular chains into consideration is one of the most practical models. In tube model, the movements of molecular chains are limited by the adjacent molecular chains, so every molecular chain is restricted in stationary space, just like a tube. Tube model can successfully explain the network structure of composites in uniaxial stress-strain condition. Moreover, the contributions of chemical cross-linking and physical entanglement to mechanical property can be separated by tube model which can also determine the value of cross-linking density [23-26].

In present work, DSC and tensile tests were used to determine oxidation onset temperature (OOT), oxidation induction time (OIT), protection factors (PF), degradation activation energy and mechanical property of SBR/silica and SBR/RT-silica composites. The results showed that RT-silica was one innovative kind of rubber antioxidant, which possessed high anti-aging efficiency, long service life, non-blooming property and outstanding reinforcement performance. What's more, the predictions for the service life of SBR composites containing non-migratory antioxidant and the changes of rubber network structure caused by nanosilica-based antioxidant during thermo-oxidative aging are reported firstly.

Experimental

Materials

Fumed silica (T40, specific surface area 400 ± 40 $m^2 g^{-1}$) with two silicon hydroxyls per square nanometer was supplied by Chenguang Research Institute of Chemical Industry (China). SBR1502 was provided by Lanzhou petrochemical company (China). Sulfur, zinc oxide (ZnO), stearic acid (SA) and N-cyclohexyl-2-benzothiazole sulfonamide (CZ) were commercial grade merchandise. RT-silica was synthesized in our laboratory and the amount of grafted antioxidant agent was 0.021 g per 1 g RT-silica.

Preparation of RT-silica

The nanosilica-immobilized antioxidant (RT-silica) was synthesized and its molecular structure was showed in Fig.1. RT (4.5 g) was dissolved in the methylbenzene (150 ml). Then KH-560 was instilled in the solution gradually and the mixed solution was stirred at 85 ℃ for 4 h. After 4 h, fumed nanosilica (10 g) was added into the mixed solution which continued to be stirred for 48 h at 100 ℃. Then the solution was filtered to obtain solid mixture. The solid mixture was dried in a vacuum oven for 10 h at 65 ℃. Finally, the solid mixture was extracted via acetone to remove the unreacted RT for 72 h. The product named as RT-silica was dried in the vacuum oven at 65 ℃ for 24 h before use.

Preparations of SBR/silica composites

The SBR composites were prepared via a two-roll mill for 10 min at room temperature. First, the raw SBR was plasticated on a two-roll mill and then SA, CZ, ZnO, silica and sulfur were added onto the mill to mix with SBR matrix evenly. This mixed rubber elastomer was placed at least for 24 h before vulcanization. Then these

elastomer mixtures containing different kinds of fillers were vulcanized at 150 ℃ under pressure of 15 MPa for t_{90} (optimum cure time) which was determined by vulcanization curves. Finally, the vulcanized rubber was tailored in an average thickness of 2 mm. The contents of ingredients of these SBR/silica composites were listed in Table.1.

Mechanical property tests

Instron 5567 material testing machine (with a 1 kN load cell) was applied to test the tensile strength and elongation at break of SBR composites at room temperature with extensional strain rate of 500 mm min^{-1} in accordance with GB/T1040-92. The initial thickness and length of the samples were 2 and 15 mm. Each test chose an average value of five parallel samples. All samples for accelerated aging test were aged in air condition at 85 ℃ for different time. The mechanical properties of the samples before and after aging were measured.

DSC tests

The anti-oxidation performances of SBR composites were tested with a TA Q200 differential scanning calorimeter. The tests were carried out in oxygen atmosphere. The oxygen flow was 50ml min^{-1}. The weight of the sample was about 8mg. Non-isothermal DSC measurements were used to study the OIT of different SBR composites, which adopt five different heating rates of 3, 5, 7, 10 and 15 K min^{-1}. The temperature-rise period lasted until the temperature reached up to 350 ℃.

Determination of non-isothermal oxidation induction time

In terms of non-isothermal DSC measurement which is performed at constant

heating rate, the relation between the oxidation onset temperature (Ti) and heating rate (β) can be described by the following equations [27-30]:

$$T_i = \frac{1}{D}\ln(AD\beta + 1) \quad (1); \quad T_i = T_\infty\left(1 - \exp(-\beta^a)\right) \quad (2)$$

where A, D are the kinetic parameters of describing the length of inducing period (IP), T_∞ is iso-conversional temperature at infinite heating rate and a is the heating rate index, separately. After A, D, T_∞ and a were calculated, the OIT value at certain temperature can be also calculated via the expressions [29-30]:

$$t_i = A\exp(-DT) \quad (3); \quad t_i = (T_\infty - T)a\left(\ln\frac{T_\infty}{T_\infty - T}\right)^{\frac{a-1}{a}} \quad (4)$$

where t_i is the value of non-isothermal OIT.

Activation energy calculation

In order to investigate the changes of degradation activation energy of SBR composites during thermal oxidation, TG experiments were carried out at heating rates of 5, 10, 20 and 30 ℃/min from room temperature to 800 ℃ in air to measure the TG curves of SBR composites. Then, based on the TG results, Kissinger–Akahira–Sunose (KAS) method and Friedman method were used to calculate the degradation activation energy. KAS method is based on the following expression [31]:

$$\ln\left(\frac{\beta}{T_\alpha^2}\right) = \ln\left(\frac{Rk_0}{E_{a,\alpha}g(\alpha)}\right) - \frac{E_{a,\alpha}}{RT_\alpha}$$

where β is the heating rate, α is the conversion of thermal degradation, T_α is the temperature at conversion of α, R is the gas constant, k_0 is the pre-exponential factor, $g(\alpha)$ is the degradation mechanism function and $E_{a,\alpha}$ is the activation energy corresponding to the conversion at α. The value of E_α can be acquired from the

slope of the fitted line of ln (β/T_α^2) against $1/T_\alpha$.

Friedman method is on the basis of the following equation [32]:

$$\ln\left(\beta\frac{d\alpha}{dT}\right) = \ln\left(Af(\alpha)\right) - \frac{E_\alpha}{RT_\alpha}$$

where β is the heating rate, α is the conversion of extent of reaction, A is the pre-exponential factor, T is the absolute temperature during reaction, R is the gas constant and E_α is the reaction activation energy. As the conversion of extent of reaction (α) is constant, $\ln\left(Af(\alpha)\right)$ is also constant. Therefore, the value of E_α can be obtained from the slope of the fitted line of $\ln\left(\beta\frac{d\alpha}{dT}\right)$ against $1/T_\alpha$.

Tube model

Tube model was applied to analyze the affection of fillers on cross-linking network of SBR composites. Based on tube model, the constitutive equation of material deformation under uniaxial stress is:

$$\sigma_M = \frac{\sigma}{\lambda-\lambda^{-2}} = G_c + G_e f(\lambda)$$

where G_C is the elasticity modulus, G_e is the entanglement modulus, σ_M is the decay stress, σ is the tensile stress and λ is the elongation of sample. This constitutive equation is mainly comprised by the contributions of G_C corresponding to the chemical cross-linking and G_e which is primarily affected by the topological constraint. Additionally, $f(\lambda)$ in the equation is defined as a deformation function that can be described by expressions [25-26]:

$$f(\lambda) = \frac{2}{\beta}\frac{\lambda^{\beta/2} - \lambda^{-\beta}}{\lambda^2 - \lambda^{-1}};\ f(\lambda = 1) = 1$$

where β is an experienced parameter that can describe the relaxation behavior of tube size at tensile stress. In general, the value of β is 1.

Because of the existence of filler in rubber matrix, the contribution of overstretched rubber matrix to mechanical property must be considered. Hence, the deformation parameter (λ) of rubber matrix must be translated into inherent deformation (λ') which can be obtained from the expression:

$$\lambda' = (\lambda - 1)\chi_{\mathrm{eff}} + 1$$

where χ_{eff} is the effective amplification factor. Moreover, χ_{eff} is able to be calculated by an equation:

$$\chi_{\mathrm{eff}} = 1 + 2.5f\varphi_{\mathrm{eff}} + 14.1f\varphi_{\mathrm{eff}}^2 = \frac{\mathrm{G}}{\mathrm{G}_0}$$

where φ_{eff} is the effective volume fraction, G_0 stands for the modulus of neat matrix, shape factor f is the length-diameter ratio of particles and G is the modulus of composites. It is evident that we have an equation: $f(\lambda) = f(\lambda')$ in unfilled rubber system.

Results and discussion

The non-isothermal oxidation induction time and protection factors of SBR/RT-silica composites

Taking SBR matrix as example, Fig.2 shows the DSC curves of SBR matrix at different heating rates, from which the oxidation onset temperature (T_i) of SBR matrix can be obtained. Thus, the T_i of SBR/RT-silica composites at different heating rates can be determined via the same method, and the results are showed in Table.2. According to the data of Table.2, the fitted curves of T_i and heating rate (β) have been respectively drawn in Fig.3 and Fig.4, and the experimental data are consistent with Equation (1) and (2), confirming that Equation (1) and Equation (2) as time

functions are indeed reliable. Additionally, A, D, T_∞ and a as the kinetic parameters of pristine SBR and SBR composites are determined from the fitting results, as shown in Table.3.

As we know, all the aspects of properties of SBR will suddenly decline after inducing period (IP), so the length of IP (t_i) is an important parameter for estimating the stability of SBR composites [33]. Based on the kinetic parameters in Table.3, t_i of SBR composites at the storage temperature of 25 ℃, the accelerated aging temperature of 85 ℃ and the processing temperature of 150 ℃ were respectively calculated via Equation (3) and Equation (4). The calculated values are listed in Table.3. It can be found that there are some differences between the calculated values of t_i of Equation (3) and (4) at ambient temperature, whereas the calculated values become more and more approximate with the rising of temperature. It is because although both Equation (3) and Equation (4) are non-Arrhenius functions, the coefficients of variability of the parameters of Equation (4) are lower, which enables Equation (4) to make more accurate prediction about IP length at ambient temperature [29].

Compared with the IP length of SBR matrix, it is clear that silica hardly increases the IP length of SBR matrix, and adversely silica shortens the IP length of SBR matrix at high temperature, indicating that silica has no anti-oxidation effect on SBR matrix, and it even plays an accelerating role on the thermo-oxidative aging of SBR in high temperature condition. Nevertheless, no matter the temperature is high or low, the IP lengths of SBR/RT-silica composites have been significantly prolonged in contrast

with SBR matrix. With the increasing of the content of RT-silica, the IP lengths of SBR/RT-silica composites get longer and longer. Based on the above analysis, RT-silica indeed possesses great anti-oxidation effect on SBR matrix.

Apart from OOT and OIT, protective factor (PF) is also one of the most commonly used parameters of measuring the stability of material, which can be calculated from OIT value of material via the equation:

$$\mathrm{PF} = \frac{t_i(\mathrm{stab})}{t_i(\mathrm{unstab})} \quad (5)$$

where t_i(stab) is the OIT value of SBR composites and t_i(unstab) is the OIT value of SBR matrix. It can be seen from Equation (5) that if the value of PF is greater than 1, the fillers have stabilization effect on SBR matrix. On the contrary, if the value of PF is less than 1, the fillers have acceleration effect on the thermo-oxidative aging of SBR matrix. In addition, the anti-oxidation efficiency of filler has a positive linear correlation with the value of PF.

Table.4 presents the calculations of PF of SBR composites at 25 ℃, 85 ℃ and 150 ℃. As can be seen from Table.4, all values of PF of SBR/RT-silica composites at different temperatures are far greater than 1, while the values of PF of SBR/silica composites fluctuate around 1. Particularly, the values of PF of SBR/silica composites are much less than 1 at high temperature, indicating that silica really makes no difference on improving the anti-aging performance of SBR composites, and it even produces an accelerating effect on aging of SBR composites at high temperature. Furthermore, at the same temperature, the PF of SBR/RT-silica composites increase with the rising of RT-silica content. As the temperature grows, the PF of SBR/RT_{10}

composites slightly reduce, the values of PF of SBR/RT_{20} composites remain almost stable and the PF of SBR/RT_{30} composites have a significant increase. Based on the analysis above, the anti-oxidation performance of SBR composite is improved with the increase of RT-silica loading contained in SBR composite, and high content of RT-silica contained in SBR composite contributes to enhance the anti-aging performance of SBR composite at high temperature.

The changes of mechanical properties of SBR composites during accelerated aging

From the stress-strain curves of pristine SBR and its composites in Fig.5, the tensile strength of the two kinds of SBR composites both increase with the rise of filler loading. When the content of filler is 10 phr, RT-silica and silica present similar reinforcement performance, but the tensile strength of SBR/RT_{20} increases to 16.6 MPa compared with 12.2 MPa of SBR/$silica_{20}$, with SBR/RT_{30} increasing to 25.1 MPa compared with 18.1 MPa of SBR/$silica_{30}$. The facts demonstrate that RT-silica has better reinforcement performance on SBR matrix. The reason why there is difference in reinforcement performance between RT-silica and silica is that the two kinds of filler possess different dispersity in SBR matrix. As the filler contents are less than 10 phr, namely, low content of fillers, both RT-silica and silica have well dispersity in SBR matrix, whereas neither of them can form effective filler network, which results in that the tensile strength of SBR/RT_{10} and SBR/$silica_{10}$ are basically similar. When both of the filler contents increase to 20 phr, which is enough to form effective filler network, the mechanical properties of SBR composites can be largely improved. However, after silica was grafted with RT, the polar Si-hydroxyl groups on the surface

of silica were replaced by non-polar diaminobenzene groups, giving rise to that the surface of silica turned to non-polar surface. The non-polar surface of RT-silica makes it disperse better than silica in SBR matrix, so that RT-silica molecules are difficult to form large aggregations in SBR composites and can form wider and more effective network than silica molecules in SBR composites. Hence, when the content of filler increases to 20 phr, the tensile strength of SBR/RT-silica composites is much higher than that of SBR/silica composites.

The difference between RT-silica and silica not only exists in the reinforcement performance on SBR matrix, but also exists in the aging resistance. Fig.6 is the histogram of tensile strength of SBR composites which are subjected to accelerated aging at 85 ℃ in a heating aging test chamber, describing the change tendency of tensile strength of SBR composites in the thermo-oxidative aging process. As mentioned above, the mechanical property of SBR/RT-silica composites is much better than that of SBR/silica composites before aging. It can be seen from Fig.6 that the tensile strength of the two kinds of SBR composites both decline with the extension of aging time. After the two kinds of SBR composites containing the same content of filler suffer from the same aging time, the tensile strength of SBR/RT-silica composite is always higher than that of SBR/silica composite. Furthermore, when the aging time of SBR composites reaches up to 22 days, the tensile strength of SBR/RT_{10} still remains 4.3 MPa, but the remaining tensile strength of SBR/$silica_{10}$ is only 2.6 MPa. The retention rates of mechanical property of SBR/RT_{20} and SBR/$silica_{20}$ which were also aged for 22 days are 54 % and 44 %, respectively. After aging for the same

time, this gap in mechanical property is more evident for SBR/RT_{30} and SBR/$silica_{30}$. In detail, the tensile strength of SBR/RT_{30} is 15 MPa, while that of SBR/$silica_{30}$ is 11 MPa.

As shown in Fig.7, the variation trend of elongation at break of SBR composites during the thermo-oxidative aging is roughly similar with that of tensile strength. After suffering from the same aging time, the elongation at break of SBR/RT-silica is always greater than SBR/silica, when the filler content of the two kinds of SBR composites are identical, indicating that SBR/RT-silica composite can keep more excellent elasticity after thermo-oxidative aging. In consequence, SBR/RT-silica composite possesses higher security and reliability than SBR/silica in severe environment.

Based on the above experimental results, it can be concluded that RT-silica can not only endow SBR composites with more advantageous mechanical property, but also makes SBR composites possess better aging resistance. Consequently, compared with traditional SBR/silica composite, SBR/RT-silica composite has better usability and higher safe factor.

Degradation Kinetics of SBR composites

Fig.8 and Fig.9 are the analysis results of TG data via KAS and Friedman method, and the analysis results of SBR matrix are listed in the illustrations of Fig.8 and Fig.9. It can be seen from Fig.8 that the vibration trends of E_a versus degradation conversion of SBR/silica composites are similar with that of SBR matrix, demonstrating that the incorporation of silica is not able to transform the

degradation mechanism of SBR matrix. As the incorporation of silica is likely to hinder the motion of polymer chains and restrict the diffusion of heat and oxygen in SBR composites, the values of Ea of SBR/silica composites are different from that of SBR matrix. But the values of Ea of SBR/RT-silica composites exhibit entirely different trend in contrast with that of SBR matrix, revealing that SBR/RT-silica composite and SBR matrix follow diverse aging mechanisms. In other words, RT-silica could alter the thermal-oxidative aging behavior of SBR matrix, which results from the phenylamine groups on the surface of RT-silica. The calculations of Ea of SBR composites via Friedman method in Fig.9 present the same change law with that of KAS method, testifying the reliability of experimental results.

Effect of RT-silica on the network structure of SBR composites during aging process

The parameters of tube model have been calculated to investigate the changes of cross-linking network during thermo-oxidative aging. By analyzing the change regularity of the parameters of tube model, the changes of cross-linking network of SBR composites with the passage of aging time can be found. Taking SBR matrix as example, the values of G_C and G_e can be got through fitting the linear part of decay stress-deformation functions of SBR matrix, as shown in Fig.10.

Table.5 and Table.6 list the change tendency of G_C and G_e which are the tube model parameters of SBR and SBR/RT-silica composites after thermo-oxidative aging at 85 ℃ for different time. It can be observed from Table.5 and Table.6 that with the incorporation of RT-silica, there is little change in the values of G_C, indicating that

RT-silica is not able to change the cross-linking density of SBR matrix. And the increase of the values of G_e shows that more chain entanglements have been induced in SBR/RT-silica composites, due to the strong physical interaction between RT-silica aggregations and rubber molecular chains. Moreover, the values of G_C of SBR and SBR/RT-silica composites both increase firstly and then decrease with the extension of aging time, while the values of G_e always increase over aging time, revealing that the incorporation of RT-silica can only restrain the deterioration of material performance resulting from thermo-oxidative aging, but it can't transform the change regularity of rubber network in the process of thermo-oxidative aging.

Conclusions

The thermo-oxidation resistance of SBR/RT-silica composites with different content of fillers was researched in this paper. According to the results of DSC test, it was clear that RT-silica can obviously prolong the oxidation induction time of SBR/RT-silica composites, though silica had acceleration effect on the thermo-oxidation degradation of SBR composites. Besides, the values of activation energy were calculated by KAS and Friedman methods. It was found that the thermal-oxidative aging behaviors of SBR and SBR/silica composites were similar, but the thermal-oxidative aging behavior of SBR/RT-silica composite was entirely different from that of pristine SBR and SBR/silica composites because of the incorporation of RT-silica. Based on the analysis of tensile tests, RT-silica can improve the mechanical property of SBR matrix more effectively than silica, and SBR/RT-silica composites possessed higher tensile strength and elongation at break than SBR/silica

composites after aging at 85 ℃, demonstrating that RT-silica restrained the deterioration of material property derived from thermal oxidation aging of SBR. In summary, as a new kind of immobile rubber antioxidant, RT-silica possessed outstanding anti-aging and reinforcement performance.

Acknowledgements

This study is financially supported by the National Science Foundation of China (Grant No. 51133005).

References

[1] Mohsen M, Salam MHA, Ashry A, Ismail A and Ismail H, Positron annihilation spectroscopy in carbon black-silica- styrene butadiene rubber (SBR) composites under deformation, *Polymer Degradation and Stability*, 2005, 87, 381-388.
[2] N. Rattanasom, T. Saowapark and C. Deeprasertkul, Reinforcement of natural rubber with silica/carbon black hybrid filler, *Polymer Testing*, 2007, 26, 369-377.
[3] M. N. Ismail, M. S. Ibrahim and M. A. A. El-Ghaffar, Polyaniline as an antioxidant and antirad in SBR vulcanizates, *Polymer Degradation and Stability*, 1998, 62(2), 337-341.
[4] M. N. Ismail, M. A. A. El-Ghaffar, K. A. Shaffei and N. A. Mohamed, Some novel polyamines as antioxidants for SBR vulcanizates, *Polymer Degradation and Stability*, 1999, 63(3), 377-383.
[5] Nikiel L, Gerspacher M, Yang H and O'Farrell C P, Filler dispersion, network density, and tire rolling resistance, *Rubber Chemistry and Technology*, 2001, 74(2), 249-259.
[6] Hertl W, Mechanism of gaseous siloxane reaction with silica Ⅰ, *The Journal of Physical Chemistry*, 1968, 72(4), 1248-1256.
[7] Hertl W, Mechanism of gaseous siloxane reaction with silica Ⅱ, *The Journal of Physical Chemistry*, 1968, 72(12), 3993-4003.
[8] Hertl W and Hair M L, Reaction of hexamethyldisilazane with silica, *The Journal of Physical Chemistry*, 1971, 75(14), 2181-2189.
[9] Khalfi A, Papirer E, Balard H, Barthel H and Heinemann M G, Characterization of Silylated Silicas by Inverse Gas Chromatography: Modelization of the Poly(dimethylsiloxane) Monomer Unit/Surface Interactions Using Poly(dimethylsiloxane) Oligomers as Probes, *Journal of Colloid and Interface Science*, 1996, 184(2), 586-593.
[10] Tsutsumi K and Takahashi H, Studies of surface modification of solids, *Colloid and Polymer Science*, 1985, 263(6), 506-511.
[11] Ismail M N, Yehia A A and Korium A A, Evaluation of some arylphosphites as antioxidants and antifatigue agents in natural rubber and styrene–butadiene rubber vulcanizates, *Polymer Degradation and Stability*, 2001, 74(2), 247-253.

[12] Baharvand H, Naderi G and Soltani S, SBR composites reinforced with N-isopropyl-N'-phenyl-p-phenylenediamine-modified clay, *Chinese Journal of Polymer Science*, 2011, 29(2), 191-196.
[13] Lili Guo, Hangxin Lei, Jing Zheng, Guangsu Huang and Guangxian Li, Synthesis of nanosilica-Based immobile antioxidant and its antioxidative efficiency in SBR Composites, *Polymer Composites*, 2013, 34(11), 1856-1862.
[14] Cibulková Z, Šimon P and Lehocký P, DSC study of the influence of p-subtituted diphenyl amines on the thermooxidative stability of styrene-butadiene rubber, *Journal of Thermal Analysis and Calorimetry*, 2010, 101(2), 679-684.
[15] Šimon P and Kolman L, DSC study of oxidation induction periods, *Journal of Thermal Analysis and Calorimetry* , 2001, 64, 813-820.
[16] Šimon P, Induction periods: theory and applications, *Journal of Thermal Analysis and Calorimetry* , 2006, 84, 263-270.
[17] Cibulková Z, Černá A and Šimon P, Stabilization effect of potential antioxidants on the thermooxidative stability of styrene–butadiene rubber, *Journal of Thermal Analysis and Calorimetry*, 2011, 105(2), 607-613.
[18] Cibulková Z, Černá A and Šimon P, DSC study of stabilizing effect of antioxidant mixtures in styrene-butadiene rubber, *Journal of Thermal Analysis and Calorimetry*, 2012, 108(2), 415-419.
[19] Beliehnleier J A, Cammenga H K, Sehneider P B and Stee A G, A simple method for determining activation energies of organic reactions from DSC curve, *Thermochimica Acta*, 1998, 310(12), 147-151.
[20] Coats A W and Redferm J P, Thermogravimetric analysis-A review, *Analyst*, 1963, 88(1052), 906-924.
[21] M. Maiti, S. Mitra, and A.K. Bhowmick, Effect of nanoclays on high and low temperature degradation of fluoroelastomers, *Polymer Degradation and Stability*, 2008, 93(1), 188-200.
[22] J. Kuljanin-Jakovljević, M. Marinovic´-Cincović, Z. Stojanović, A. Krkljes, N.D. Abazovic´, and M.I. Čomor, Thermal degradation kinetics of polystyrene/cadmium sulfide composites, *Polymer Degradation and Stability*, 2009, 94(6), 891-897.
[23] Kuhn W and Grun F, Relations between elastic constants and the strain birefringence of high-elastic substances, *Kolloid Zh*, 1942, 101, 248-271.
[24] James H and Guth E, Theoretical stress-strain curve for rubberlike materials, *Physical Review*, 1941, 2(69), 111-115.
[25] Marrucci G, Rubber elasticity theory, A network of entangled chains, *Macromolecules,* 1981, 14(2), 434-442.
[26] Edwards S F and Vilgis T A, The tube model theory of rubber elasticity, *Reports on Progress in Physics*, 1988, 51(2), 243-297.
[27] Šimon P, Hynek D and Malíková M, Extrapolation of accelerated thermooxidative tests to lower temperatures applying non-Arrhenius temperature functions, *Journal of Thermal Analysis and Calorimetry*, 2008, 93(3), 817-821.
[28] Šimon P, Single-step kinetics approximation employing non-Arrhenius temperature functions, *Journal of Thermal Analysis and Calorimetry*, 2005, 79(3), 703-708.

[29] Šimon P, Material stability predictions applying a new non-Arrhenius temperature function, *Journal of thermal analysis and calorimetry*, 2009, 97(2), 391-396.
[30] Vizárová K, Reháková M and Kirschnerová S, Stability studies of materials applied in the restoration of a baroque oil painting, *Journal of Cultural Heritage*, 2011, 12(2), 190-195.
[31] Šimon P, Isoconversional methods-Fundamentals, meaning and application, *Journal of Thermal Analysis and Calorimetry*, 2004, 76, 123-132.
[32] Henry L Friedman, New methods for evaluating kinetic parameters from thermal analysis data, *Journal of polymer science part B*, 1969, 7(1), 41-46.
[33] Pospíšil J, Horák J, Pilař J, Billingham NC, Zweifel H and Nešpůrek S, Influence of testing conditions on the performance and durability of polymer stabilisers in thermal oxidation, *Polymer Degradation and Stability*, 2003, 82(2), 145-162.

Table 1 Ingredients of SBR/silica composites

System	SBR /phr	ZnO/ phr	SA / phr	CZ /phr	sulfur/ phr	silica /phr	RT-silica/ phr
Pristine SBR	100	4	2	1	2	--	--
SBR/silica$_{10}$	100	4	2	1	2	10	--
SBR/silica$_{20}$	100	4	2	1	2	20	--
SBR/silica$_{30}$	100	4	2	1	2	30	--
SBR/RT$_{10}$	100	4	2	1	2	--	10
SBR/RT$_{20}$	100	4	2	1	2	--	20
SBR/RT$_{30}$	100	4	2	1	2	--	30

Table.2 Oxidation onset temperature (Ti) at different heating rates for SBR and its composites

Sample	Ti (℃)				
Heating rate(℃/min)	3	5	7	10	
SBR	178.0	183.3	186.5	192.3	194.9
SBR/RT$_{10}$	180.7	186.8	189.9	194.5	198.6
SBR/RT$_{20}$	186.2	191.9	196.7	200.4	204.5
SBR/RT$_{30}$	200.3	206.4	210.5	215.5	220.8
SBR/silica$_{10}$	171.1	177.4	179.3	184.3	190.3
SBR/silica$_{20}$	174.8	180.2	184.8	188.6	191.5
SBR/silica$_{30}$	174.4	179.5	185.2	188.4	193.3

Table.3 Kinetic parameters A,D and T∞,a and IP lengths at 25, 85 and 150℃

Sample	A/min	D/K^{-1}	T∞/K	a	ti(25℃)/year		ti(85℃)/day		ti(150℃)/min	
					Eq(3)	Eq(4)	Eq(3)	Eq(4)	Eq(3)	Eq(4)
SBR	$5.01 \cdot 10^{17}$	0.087	694	0.045	2.6	1.9	9.3	9.0	44.2	44.5
SBR/RT$_{10}$	$1.68 \cdot 10^{18}$	0.089	699	0.043	4.6	3.3	14.3	13.6	58.0	58.5
SBR/RT$_{20}$	$7.51 \cdot 10^{17}$	0.086	707	0.044	5.2	3.6	18.2	17.2	88. 2	89. 1
SBR/RT$_{30}$	$1.19 \cdot 10^{17}$	0.080	728	0.046	6.6	4.4	31.7	29.2	229.1	232.1
SBR/silica$_{10}$	$3.56 \cdot 10^{18}$	0.093	686	0.042	3.1	2.3	8.2	8.0	27.0	27. 1
SBR/silica$_{20}$	$7.36 \cdot 10^{17}$	0.088	689	0.044	2.3	1.8	7.8	7.5	33.5	33.7
SBR/silica$_{30}$	$2.08 \cdot 10^{18}$	0.091	689	0.043	3.2	2.3	9.2	8.8	33.6	33.7

Table.4 Protection factors (PF) of SBR and its composites based on two non-Arrhenius temperature functions

Sample	PF (25℃)		PF (85℃)		PF (150℃)	
	Eq(6)	Eq(7)	Eq(6)	Eq(7)	Eq(6)	Eq(7)
SBR/RT_{10}	1.77	1.74	1.54	1.51	1.31	1.31
SBR/RT_{20}	2	1.89	1.96	1.91	2	2
SBR/RT_{30}	2.54	2.32	3.41	3.24	5.18	5.22
SBR/$silica_{10}$	1.19	1.21	0.88	0.89	0.61	0.61
SBR/$silica_{20}$	0.88	0.95	0.84	0.83	0.76	0.76
SBR/$silica_{30}$	1.23	1.21	0.99	0.98	0.76	0.76

Table.5 Gc values (MPa) of SBR and SBR/RT-silica composites

Aging time / Sample	0d	5d	10d	14d	18d	22d
SBR	0.30	0.41	0.49	0.34	0.27	0.23
SBR/RT_{10}	0.29	0.46	0.49	0.36	0.33	0.22
SBR/RT_{20}	0.34	0.45	0.59	0.42	0.34	0.26
SBR/RT_{30}	0.34	0.43	0.63	0.41	0.41	0.4

Table.6 Ge values (MPa) of SBR and SBR/RT-silica composites

Aging time / Sample	0d	5d	10d	14d	18d	22d
SBR	0.73	1.02	1.1	1.32	1.57	1.66
SBR/RT_{10}	1.06	1.44	1.26	1.65	1.53	1.77
SBR/RT_{20}	1.05	1.18	1.28	1.56	1.89	1.83
SBR/RT_{30}	1.15	1.56	1.6	1.81	1.96	2.00

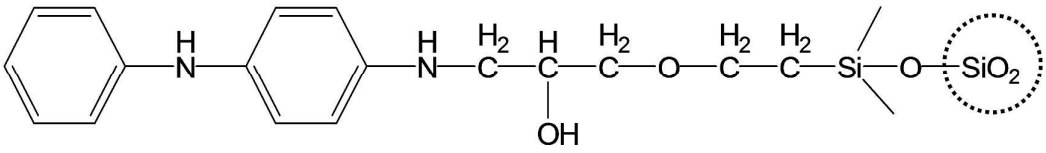

Fig.1 structure of RT-silica

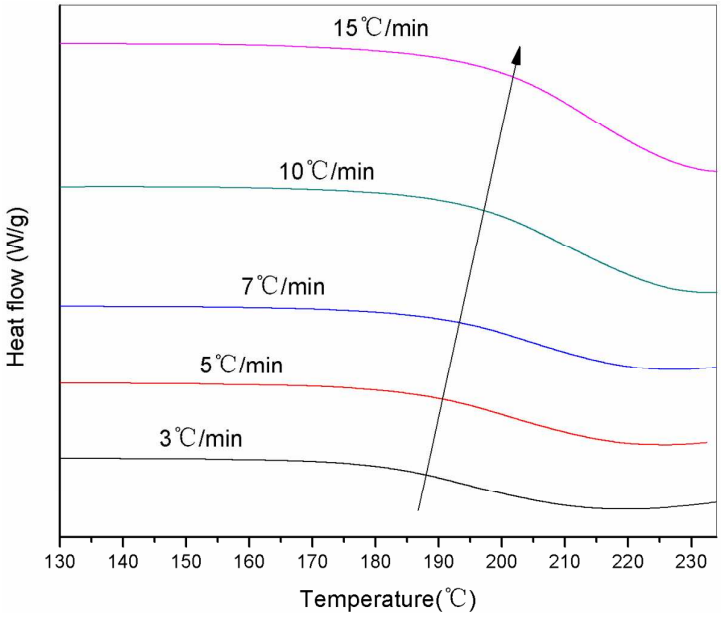

Fig.2 DSC curves of SBR at different heating rates

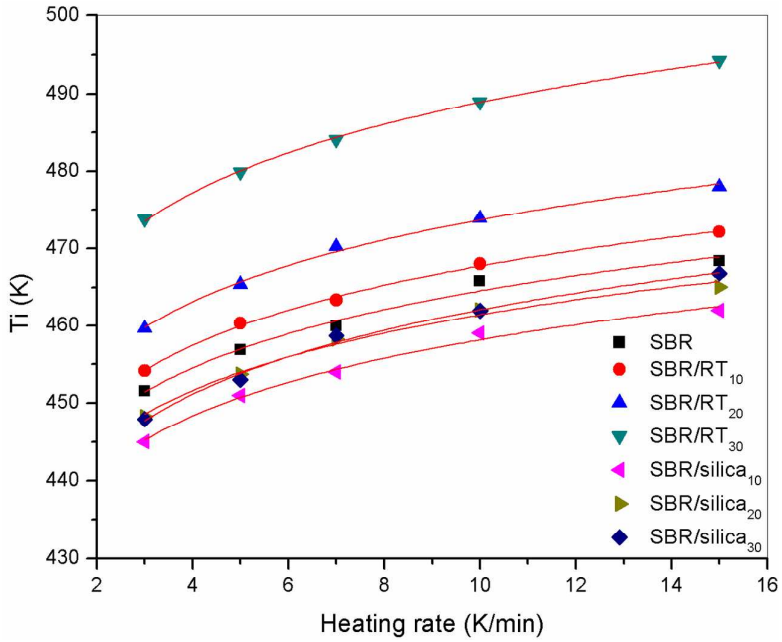

Fig.3 Fitting curves of Ti based on Eq (1). Dotted lines represent experimental data and solid lines are fitting curves

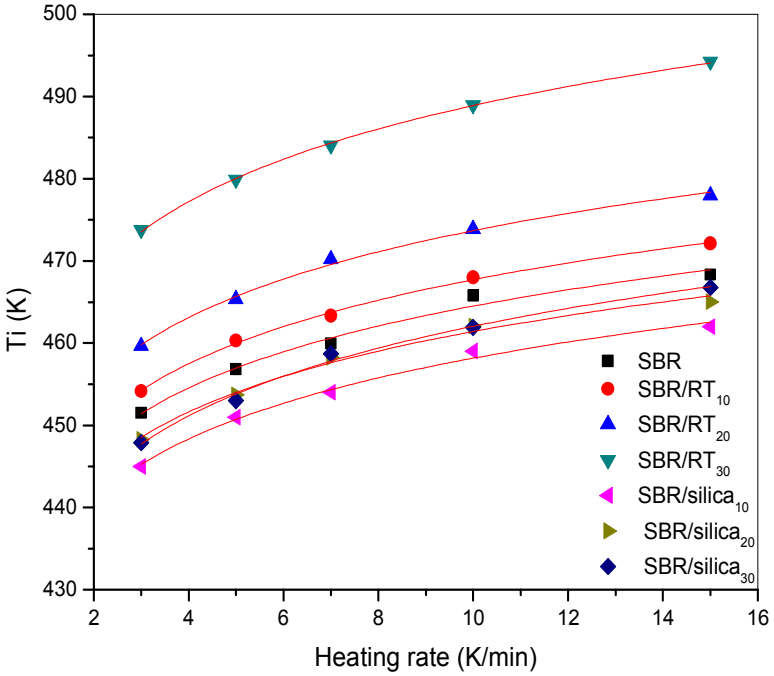

Fig.4 Fitting curves of Ti based on Eq (2). Dotted lines represent experimental data and solid lines are fitting curves

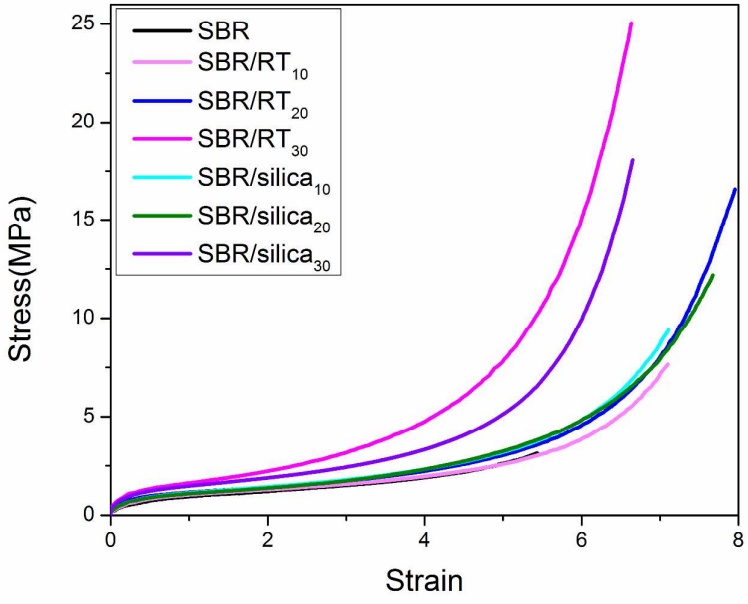

Fig.5 Stress curves of pristine SBR and its composites

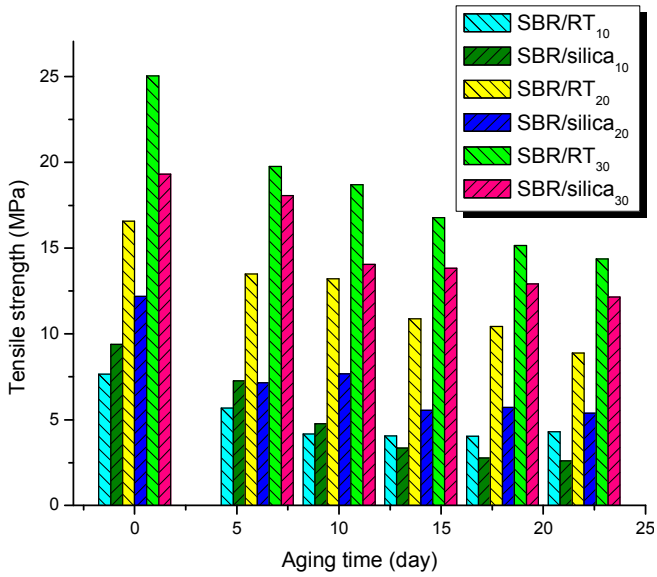

Fig.6 Tensile strength of pristine SBR and its composites after aging at 85℃ for different time

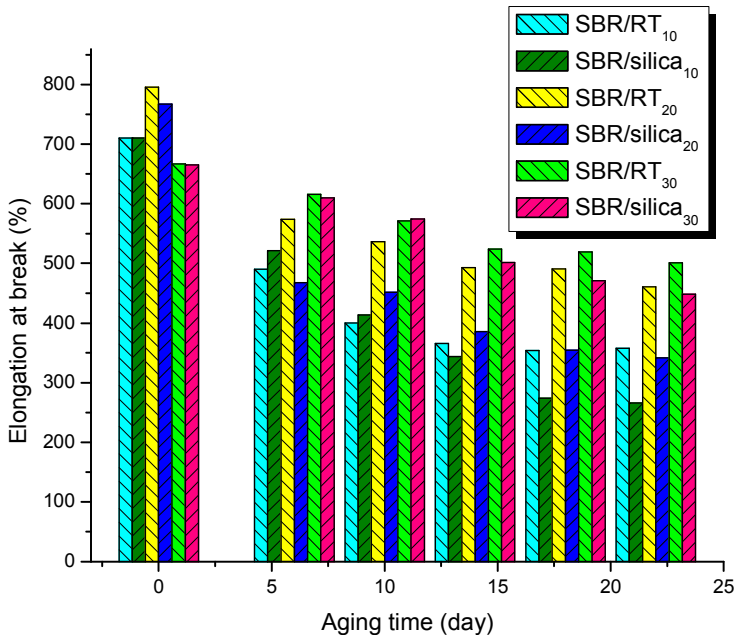

Fig.7 Elongation at break of pristine SBR and its composites after aging at 85℃ for different time

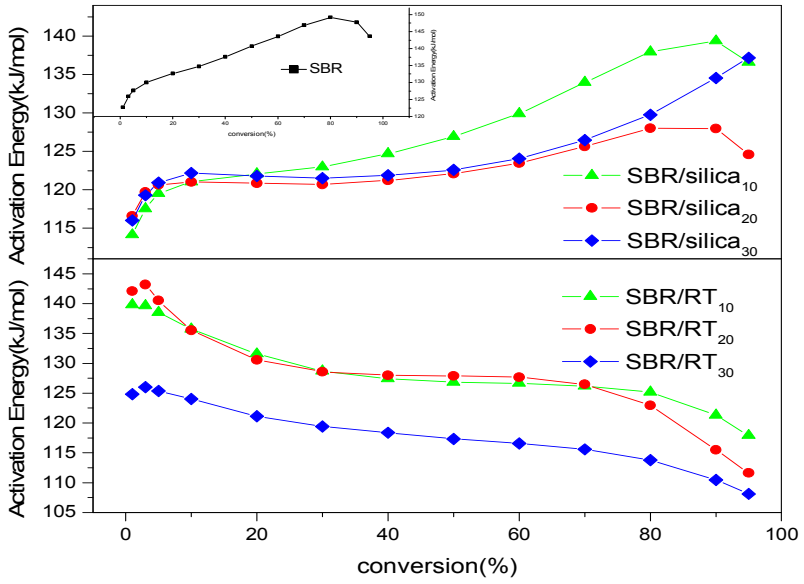

Fig.8 Activation energy versus degradation conversion based on KAS method

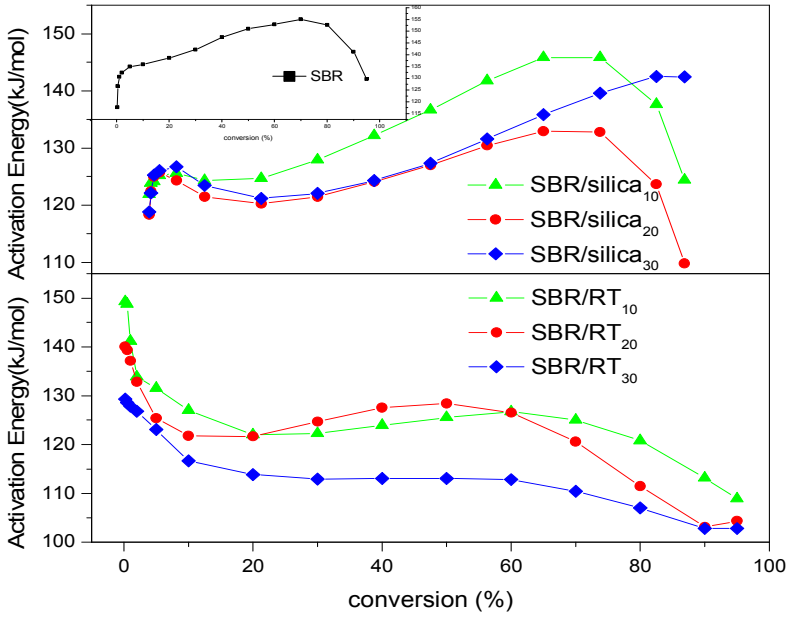

Fig.9 Activation energy versus degradation conversion based on Friedman method

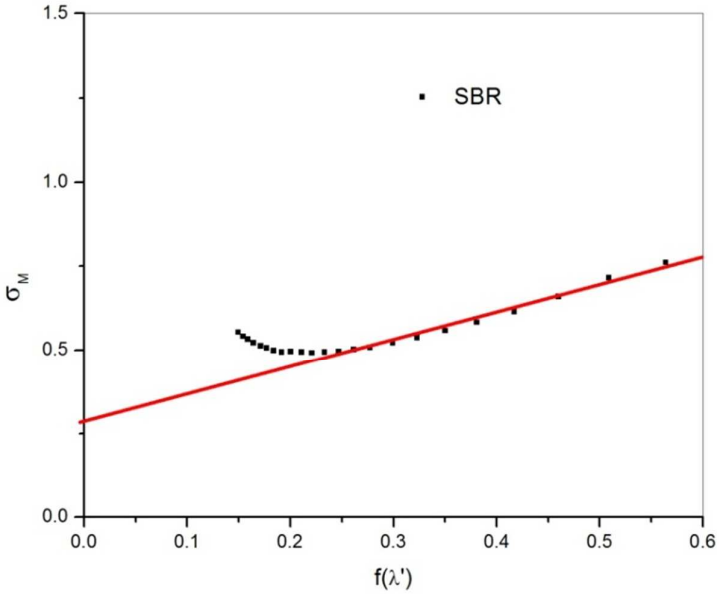

Fig.10 Determination of Gc and Ge of SBR for example